Abdominal Radiology



Abdom Radiol (2017)
DOI: 10.1007/s00261-017-1263-8

# Does intravoxel incoherent motion reliably stage hepatic fibrosis, steatosis, and inflammation?

Kumaresan Sandrasegaran,[1] Paul Territo,[1] Reem M. Elkady,[1,2] Yuning Lin,[1,3] Pauley Gasparis,[1] Gitasree Borthakur,[1] Chen Lin[1]

[1]Department of Radiology, Indiana University School of Medicine, 550 N University Blvd, UH 0279, Indianapolis, IN 46202, USA
[2]*Present address:* Department of Radiology, Assiut University, Assiut, Egypt
[3]*Present address:* Department of Radiology, Fuzhou General Hospital, Fuzhou, China

## Abstract

*Objective:* To investigate the usefulness of intravoxel incoherent motion (IVIM) in determining the severity of hepatic fibrosis, steatosis, and inflammation in patients with chronic liver disease.

*Methods:* Forty-nine patients who had liver MRI with IVIM sequence and liver biopsy within three months of MRI were enrolled. A reviewer, blinded to histology, placed regions of interest of 1–2 $cm^2$ in the right liver lobe. In addition, the first twenty patients were assessed with a second reviewer. Perfusion fraction (f), pseudodiffusion coefficient ($D_{fast}$), true diffusion coefficient ($D_{slow}$), and apparent diffusion coefficient (ADC) were calculated from normalized signal intensities that were fitted into a biexponential model. Errors in the model were minimized with global stochastic optimization using Simulated Annealing. ANOVA with post hoc Tukey–Kramer test and multivariate generalized linear model analysis were performed, using histological findings as the gold standard.

*Results:* The most common etiologies for liver disease were hepatitis C and alcohol, accounting together for 76% (37/49) of patients. Low-grade fibrosis (F0, F1), hepatic steatosis, and inflammation were seen in 24% (12/49), 31% (15/49), and 29% (14/49) of patients, respectively. The interobserver correlation was poor for $D_{fast}$ and $D_{slow}$ (0.105, 0.173) and moderate for f and ADC (0.461, 0.418). ANOVA showed a strong inverse association between $D_{fast}$ and liver fibrosis grade ($p = 0.001$). A weak inverse association was seen between ADC and hepatic steatosis ($p = 0.059$). Multivariate general linear model revealed that the only significant association between IVIM parameters and pathological features was between $D_{fast}$ and fibrosis. On ROC curve analysis, $D_{fast} < 23.4 \times 10^{-3}$ $mm^2/s$ had a sensitivity of 82.8% and a specificity of 64.3% in predicting high-grade fibrosis.

*Conclusion:* $D_{fast}$ has the strongest association with hepatic fibrosis but has weak interobserver correlation. IVIM parameters were not significantly associated with hepatic inflammation or steatosis.

**Key words:** MRI—Hepatic fibrosis—Hepatic steatosis—Hepatitis—IVIM

Hepatic fibrosis is a wound-healing response to chronic liver injury. Left untreated, fibrosis may progress to irreversible cirrhosis and complications such as portal hypertension, hepatic encephalopathy, and hepatocellular carcinoma (HCC). However, progression of early fibrosis is potentially reversible by antifibrotic therapy or by the removal of the offending etiology [1, 2]. Thus, early detection and staging of hepatic fibrosis is important for prognosis and determining need for intervention, e.g., with antiviral therapy or commencement of screening for HCC. Liver biopsy is considered the gold standard for determining the stage of hepatic fibrosis. However, this reference standard has several drawbacks, including procedural complications, sampling errors, and interobserver variation in classifying liver fibrosis. Employment of noninvasive tools in diagnosing and monitoring hepatic fibrosis has been a focus of substantial research.

Several MRI techniques have been used to study hepatic fibrosis, including diffusion-weighted imaging (DWI), dynamic contrast-enhanced MR, hepatobiliary

*Correspondence to:* Kumaresan Sandrasegaran; *email:* ksandras@iupui.edu

Published online: 21 August 2017

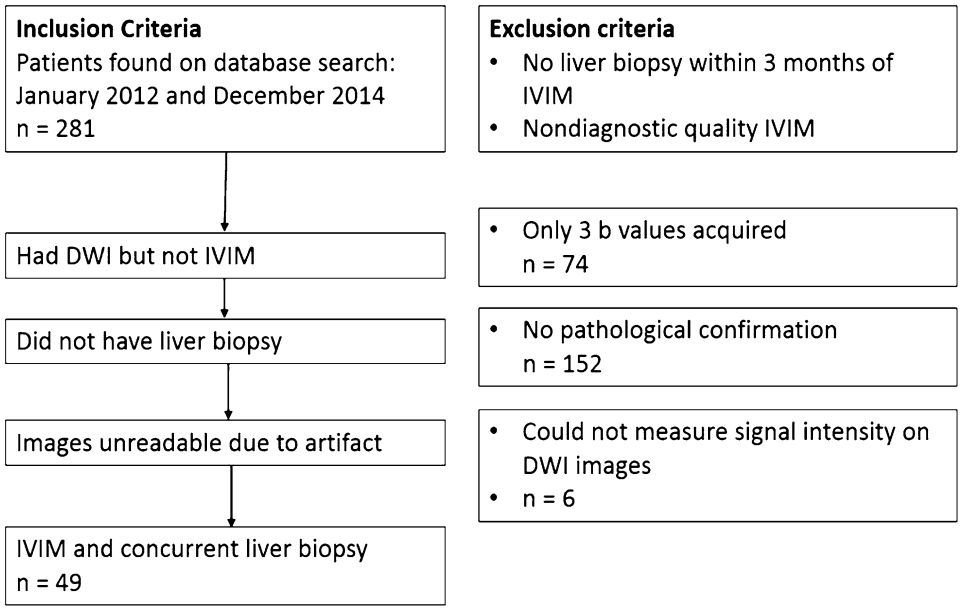


**Fig. 1.** Inclusion and exclusion criteria and derivation of study cohort.

phase parenchymal enhancement seen on gadoxetic acid-enhanced MR, and MR elastography [3–9]. Among these techniques, DWI was particularly interesting because it was hoped that excessive extracellular accumulation of collagen, glycosaminoglycans, and proteoglycans would restrict molecular diffusion of water and result in lower apparent diffusion coefficient (ADC) values than normal liver parenchyma [10]. However, it has been found that ADC cannot be reliably used to distinguish between different intermediate stages of hepatic fibrosis [11–14].

In 1986, Le Bihan et al. [15] proposed the principles of intravoxel incoherent motion (IVIM). This technique uses a more sophisticated approach to diffusion-weighted imaging to separately determine tissue diffusivity and tissue microperfusion [16]. Since altered blood perfusion occurs in chronic liver disease, perfusion parameters may also be a surrogate marker for the severity of liver fibrosis. A few studies have been conducted to correlate the IVIM parameters with the degree of hepatic fibrosis [3, 17–23]. Most prior studies did not assess for inter-observer variation in IVIM parameters or for the effect of liver fat and inflammation on these parameters. In addition, many of these studies predominantly included patients with hepatitis B, which is not a common cause of liver fibrosis in the Western population. In this study, we investigated whether IVIM-derived parameters may be used reliably as a noninvasive tool for staging hepatic fibrosis, inflammation, and steatosis.

## Methods

### *Patients*

For this retrospective Health Insurance Portability and Accountability Act (HIPAA)-compliant study, the radiology database was searched for MRI examinations with diffusion-weighted imaging (DWI) performed between January 2012 and December 2014. Institutional review board permission was obtained for retrospective assessment of imaging and clinical data with waiver of informed consent. Initial search revealed 281 patients. Forty-nine patients with diagnostic quality IVIM images and concurrent liver biopsy were included in the study. The exclusion criteria and the derivation of the study cohort are shown in Fig. 1.

### *MRI technique*

MRI examinations were performed using a 1.5 T MRI scanner (Magnetom Avanto, Siemens, Erlangen, Germany). MRI parameters are listed in Table 1. For IVIM, transverse echo-planar imaging was performed using a 6-element phased-array body coil combined with a phased-array spine coil. Frequency-selective fat saturation was used to reduce off-resonance artifacts. Parallel imaging was performed with generalized autocalibrating partially parallel acquisitions (GRAPPA) with an acceleration factor (r) of 2. Respiratory triggering was undertaken and the typical acquisition times were 12 to 15 min. Diffusion-weighted imaging was undertaken with the *b* values of 0, 50, 100, 300, 600, and 800 s/mm$^2$.

### *Image evaluation and post-processing*

Image analysis was performed by an author with 6 years' experience of viewing DWI images, and who was blinded to clinical findings and radiological follow-up. Three regions of interest (ROI) of 1–2 cm$^2$ were placed in the right liver lobe avoiding areas of artifact, vessels, and

**Table 1.** MRI parameters

| | TR/TE (ms) | Flip angle (degrees) | ST/SG (mm) | NEX | RBW | Matrix |
|---|---|---|---|---|---|---|
| T1-weighted gradient echo | 123/2.2 or 4.93[a] | 70 | 7.0/0.7 | 1 | 445 | 256 × 135 |
| T2-weighted HASTE | 1110/95 | 150 | 5.0/6.0 | 1 | 475 | 256 × 192 |
| T1-weighted fat-suppressed 3-dimensional gradient echo[b] | 4.98/2.27 | 12 | 3.0/– | 1 | 300 | 256 × 144 |
| Diffusion-weighted imaging[c] | 1500/71 | 90 | 6.0/7.8 | 4 | 1735 | 192 × 115 |

*TR* repetition time, *TE* echo time, *ST* slice thickness, *SG* gap between slices, *NEX* number of excitations, *RBW* receiver bandwidth in Hz/pixel, *HASTE* half-Fourier acquisition single-shot turbo spin echo
[a] Echo time of 2.2 ms for out-of-phase, 4.93 ms for in-phase
[b] Performed before and after intravenous gadolinium
[c] Please see text for *b* values

masses. The ROIs were placed on different slices. The left lobe was not used because of cardiac motion artifacts that can potentially alter the diffusion measurement [23]. After obtaining three ROI values, the mean value was extracted and recorded for secondary analysis. A second reviewer performed the same measurements for the first 20 patients in the cohort.

Signal intensity associated with multiple b values was modeled for IVIM according to established methods [19, 20, 22]. To account for receiver gain differences between subjects and reviewer, MRI mean intensity values $I(i, r)$, were normalized according to the following:

$$I_{\mathrm{n}}(i,r) = \frac{I(i,r)}{\mathrm{Max}(I(i,r))}, \tag{1}$$

where $I_{\mathrm{n}}$, $I$, $r$, and $i$ are the normalized signal intensity, non-normalized signal intensity, "$i$'th" subject, and "$r$'th" reviewer, respectively. Normalized data (i.e., [0.0, 1.0]) were modeled using the following functional form:

$$\begin{aligned} y(b,i,r) = {} & P_{\mathrm{f}}(i,r) * e^{-b*D_{\mathrm{f}}(i,r)} \\ & + (1 - P_{\mathrm{f}}(i,r)) * e^{-b*D_{\mathrm{s}}(i,r)}; D_{\mathrm{s}} \ll D_{\mathrm{f}}, \end{aligned} \tag{2}$$

where $y$, $P_{\mathrm{f}}$, $b$, $D_{\mathrm{f}}$, $D_{\mathrm{s}}$, $i$, and $r$ are the modeled fit, perfusion fraction, $b$ value, fast diffusion (i.e., pseudodiffusion) coefficient associated with incoherent microcirculation within the voxel, slow diffusion (i.e., true diffusion) coefficient representing pure molecular diffusion, "$i$'th" subject, and "$r$'th" reviewer, respectively. In all cases, the unweighted sum of squares error was minimized (tolerance 1e−12) via global stochastic optimization using Simulated Annealing [24].

## *Reference standard*

The histopathological assessment of liver biopsy by expert hepatopathologists was used as the reference standard. Liver fibrosis was graded as F0, F1, F2, F3, F4 as per previously published scoring system [25]. Inflammation was graded as None, Mild, and Severe and fat content was graded as Normal (<5%), Mild (5–33%), and Moderate/Severe (>33%) using previously established criteria [18, 26].

**Table 2.** Patient characteristics

| Characteristic | Number of patients ($n$ = 49) |
|---|---|
| Age (mean, range—in years) | 56.6 (32–73) |
| Gender | |
| Male | 35 |
| Female | 14 |
| Fibrosis stage | |
| 0 | 4 |
| 1 | 8 |
| 2 | 2 |
| 3 | 9 |
| 4 | 26 |
| Inflammation score | |
| None | 35 |
| Mild | 11 |
| Severe | 3 |
| Fat content | |
| None | 34 |
| Mild (5–33%) | 9 |
| Moderate and severe (>33%) | 6 |
| Etiology of liver disease[a] | |
| Hepatitis C | 35 |
| Hepatitis B | 3 |
| Alcohol | 24 |
| Autoimmune | 4 |
| Other | 7 |
| Presence of portal hypertension on MRI | |
| None | 29 |
| Yes | 20 |

[a] Some patients had more than 1 etiology for liver disease

## *Statistical analysis*

The correlation between the IVIM parameters obtained by the two reviewers (for subset of patients with two reviewers) was calculated using Spearman's coefficient. The mean and standard deviation of IVIM parameters were calculated for high-grade versus low-grade fibrosis and those with different grades of hepatic steatosis or inflammation. Low-grade fibrosis signified fibrosis staged as F0 or F1. One-way analysis of variance with post hoc Tukey–Kramer test was performed to determine differences in IVIM parameters between the groups for each histological feature. A multivariate generalized linear

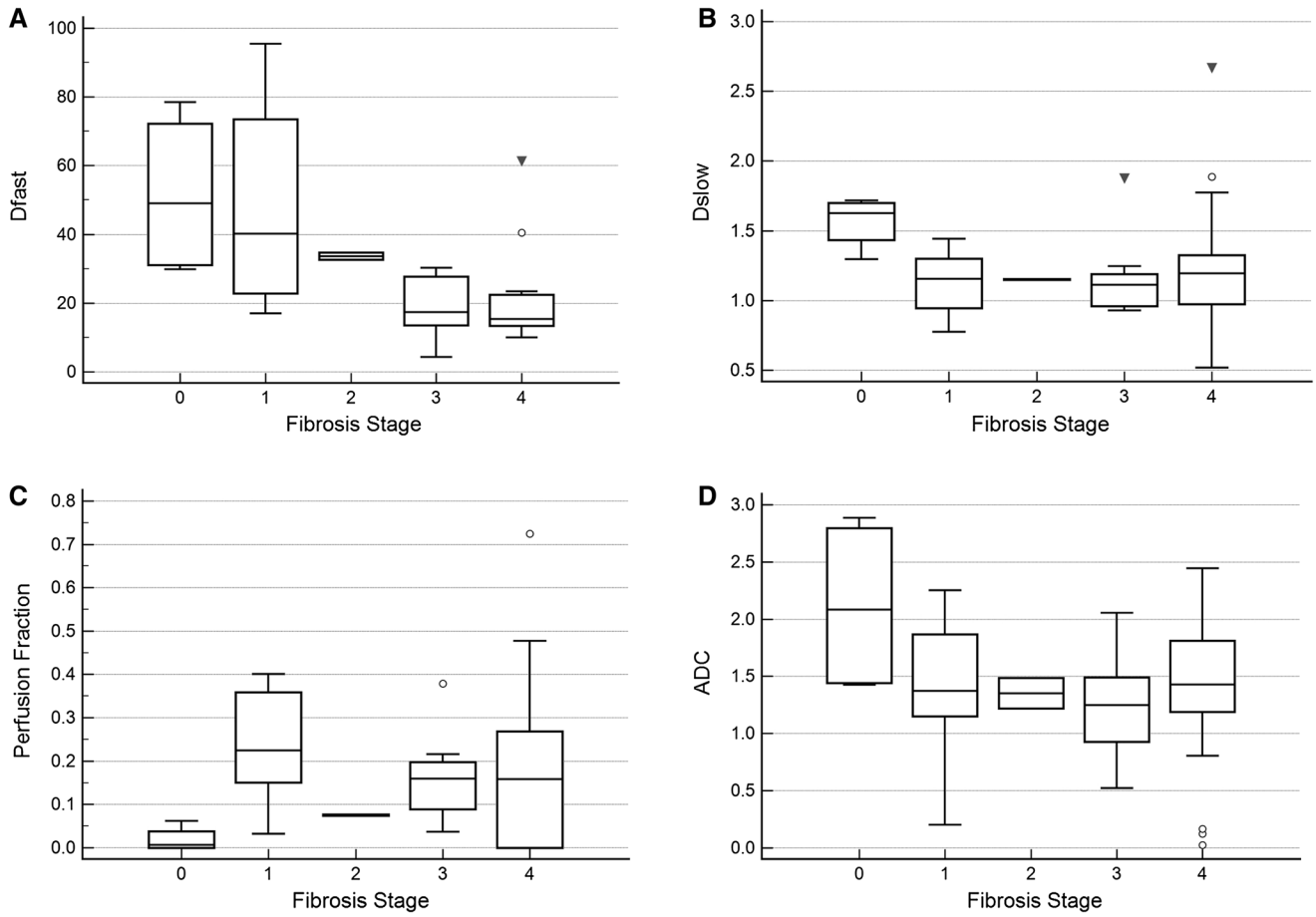


**Fig. 2.** Box-and-whisker plots for distribution of **A** $D_{fast}$, **B** $D_{slow}$, **C** perfusion fraction (*f*), and **D** ADC by histological fibrosis stages. Boxes represent the interquartile range. Whiskers represent the range of all values. *Horizontal line* within box is the median value. *Circles* and *triangles* refer to outliers.

model was created using IVIM parameters as variables to predict the grades of hepatic fibrosis, fat content, and severity of inflammation. Receiver operating characteristic curve analysis was performed to determine the area under the curve for each IVIM parameter in patients with low- versus high-grade fibrosis. A $p$ value less than 0.05 was used to indicate statistical significance. Statistical analysis was performed using MedCalc 11.1 (MedCalc Software, Mariakerke, Belgium) (for ROC curves) and PASW 18.0. (SPSS Inc, Chicago, Ill).

## Results

### *Patients*

The patients' epidemiology and liver disease are shown in Table 2. The most common etiologies for liver disease were hepatitis C and alcohol, accounting together for 76% (37/49) of cases. Low-grade fibrosis was seen in 24% of patients (12/49), while 37 patients had F2 to F4 fibrosis. Hepatic steatosis was seen in 31% of patients (15/49) and inflammation was present in 29% (14/49) of patients.

### *Association of IVIM results and histological findings*

The Spearman correlation coefficients between the two reviewers for $D_{fast}$, $D_{slow}$, perfusion fraction (*f*), and ADC were 0.105, 0.173, 0.461, and 0.418, respectively. These correlations were weak (for $D_{slow}$ and $D_{fast}$) and moderate for ADC and f. Figure 2a–d shows the box-and-whisker plots of the IVIM parameters for different stages of fibrosis. There was a substantial overlap in the values of $D_{fast}$, $D_{slow}$, f, and ADC for the different grades of fibrosis.

Table 3 shows the mean and standard deviation of IVIM parameters for patients with different histological findings together with the results of one-way ANOVA. There was a strong association between $D_{fast}$ and the degree of liver fibrosis ($p = 0.001$). Lower values of $D_{fast}$

**Table 3.** IVIM parameters

| Fibrosis | $D_{fast}$ | $D_{slow}$ | $f$ | ADC |
|---|---|---|---|---|
| Low-grade fibrosis ($n$ = 12) | 54.5 (41.6) | 1.273 (0.302) | 0.165 (0.149) | 1.642 (0.738) |
| High-grade fibrosis ($n$ = 37) | 35.4 (36.9) | 1.222 (0.352) | 0.162 (0.154) | 1.422 (0.615) |
| $p$ value* | **0.001** | 0.672 | 0.765 | 0.201 |
| No steatosis (<5%) ($n$ = 34) | 32.9 (35.9) | 1.226 (0.364) | 0.151 (0.165) | 1.489 (0.591) |
| Mild steatosis (5–33%) ($n$ = 9) | 46.6 (44.4) | 1.182 (0.322) | 0.163 (0.119) | 1.417 (0.610) |
| Moderate/severe steatosis (>33%) ($n$ = 6) | 22.6 (0.7) | 1.320 (0.421) | 0.286 (0.096) | 0.649 (0.555) |
| $p$ value* | 0.475 | 0.764 | 0.261 | 0.059 |
| No inflammation ($n$ = 35) | 28.3 (32.6) | 1.296 (0.349) | 0.122 (0.091) | 1.747 (0.576) |
| Mild inflammation ($n$ = 11) | 40.9 (39.4) | 1.231 (0.264) | 0.177 (0.176) | 1.155 (0.618) |
| Severe inflammation ($n$ = 3) | 32.2 (37.0) | 1.174 (0.448) | 0.164 (0.153) | 1.584 (0.515) |
| $p$ value* | 0.645 | 0.634 | 0.620 | 0.127 |

$D_{slow}$ slow diffusion (in $10^{-3}$ mm$^2$ /s), $D_{fast}$ fast diffusion (in $10^{-3}$ mm$^2$ /s), $f$ perfusion fraction, $ADC$ apparent diffusion coefficient (in $10^{-3}$ mm$^2$ /s)
* $p$ values from one-way ANOVA with post hoc Tukey–Kramer test

were seen in high-grade fibrosis. A weaker association ($p$ = 0.059) was also seen between ADC and hepatic steatosis, with ADC trending lower as hepatic fat content increased.

Multivariate general linear model determined the effect of IVIM parameters on multiple variables—fibrosis, fat, and inflammation. The only significant result of this model was an association between $D_{fast}$ and fibrosis ($p$ = 0.023). All other IVIM parameters were not found to be significantly associated with any histological finding.

Receiver operating characteristics analysis results are shown in Fig. 3. $D_{fast}$ had the highest, but not significantly higher, area under the curve of the IVIM parameters. A $D_{fast}$ value of less than 23.4 × $10^{-3}$ mm$^2$/s had a sensitivity of 82.8% and a specificity of 64.3% in predicting high-grade fibrosis.

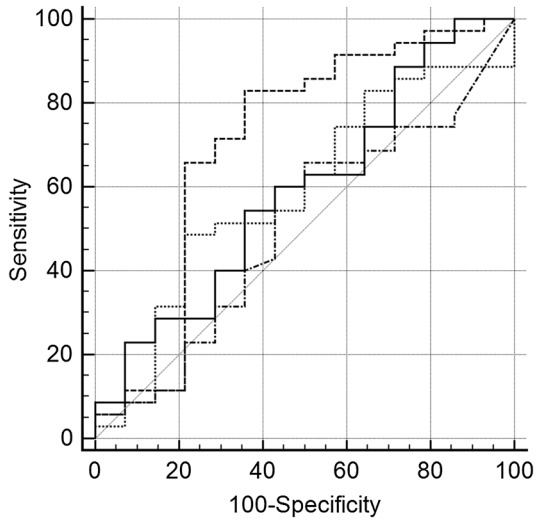


**Fig. 3.** Receiver operating characteristic (ROC) curves of IVIM parameters for differentiating between high- and low-grade fibrosis. *Dashed curve* represents $D_{fast}$. *Dotted curve* represents $D_{slow}$. *Dot-dashed curve* represents perfusion fraction. *Solid curve* represents ADC measurements. *Diagonal line* represents the area under the curve (AUC) of 0.50. The mean AUC (95% confidence interval) values for $D_{fast}$, $D_{slow}$, perfusion fraction, and ADC were 0.706 (0.559–0.828), 0.586 (0.436–0.725), 0.505 (0.359–0.651), and 0.590 (0.359–0.651), respectively.

## Discussion

Several studies have investigated the use of diffusion-weighted MRI in hepatic fibrosis staging. Most of these studies concluded that ADC values significantly decreased in cirrhotic liver as compared with normal liver [7, 8, 12, 27–32]. There was a general trend in the reduction of ADC with increasing severity of fibrosis, but there was a substantial overlap in the range of ADC values for F1 to F4 fibrosis. Most studies did not find a correlation between fibrosis staging and ADC values [7, 30–32], especially for grading intermediate stages of fibrosis [12, 33]. Issues that cause differences in findings between these studies include the lack of a standardized imaging protocol and the confounding effects of inflammation and steatosis [12, 13, 30, 33].

It is well known that perfusion contributes to ADC changes that occur in chronic liver disease. A study on rats suggested that microcapillary perfusion changed to a greater extent than diffusion in liver injury caused by carbon tetrachloride [34]. IVIM was introduced as a technique to separate the diffusion- and perfusion-related parameters [35]. IVIM postulates that the signal attenuation with increasing $b$ values may be expressed by a biexponential, instead of a mono-exponential, equation and gives rise to three additional parameters: perfusion-related diffusion ($D_{fast}$, also known as pseudodiffusion coefficient or fast diffusion coefficient), perfusion fraction (f), and pure diffusion coefficient ($D_{slow}$, also known as true diffusion coefficient or slow diffusion coefficient) [36]. Prior studies have evaluated the role of IVIM in staging of liver fibrosis [3, 17–23]. Some studies evaluated the difference between cirrhotic patients and normal control population [20, 21], without assessing intermediate grades of fibrosis. Most studies did not assess

interobserver correlation [3, 17, 19–23]. In addition, in several studies a substantial number of patients had hepatitis B or the etiology of diffuse liver disease was not given [17, 19, 20, 22, 23].

We analyzed a subset of our patients with two reviewers and found that the correlation between some IVIM parameters, particularly $D_{fast}$, was weak. The poor reproducibility of $D_{fast}$ has been shown by prior studies [37–39]. The weak interobserver correlation creates difficulty in making definite conclusions about the association of liver fibrosis and IVIM parameters. Our main finding was a strong association between hepatic fibrosis and $D_{fast}$. This agrees with the findings of prior studies [3, 17, 19, 22, 23]. A meta-analysis of the association between IVIM parameters and hepatic fibrosis also suggested that $D_{fast}$ is the best IVIM parameter [40]. However, two caveats need to be noted. The interobserver correlation of $D_{fast}$ is weak. There is also a substantial overlap in $D_{fast}$ values between intermediate grades of fibrosis, making it less valuable in individual patients.

We assessed the effect of fat and inflammation on IVIM results. We did not find a significant association between IVIM parameters and these histological features; the ADC values were reduced in patients with moderate or severe hepatic steatosis ($p = 0.059$). This finding is consistent with prior studies on DWI [41, 42].

We are aware of some limitations of our study. The study was retrospective and the number of subjects in the cohort ($n = 49$) was small. Histology was used as a reference standard, though as discussed previously biopsy results may not be a true gold standard. We used six $b$ values in our study, instead of the more usual 10–12 values. In routine clinical practice, time constraints make it difficult to perform diffusion-weighted sequences with numerous $b$ values. A recent study [43] showed that adequate IVIM results may be obtained using only 3 "low" $b$ values, i.e., less than 100 s/mm$^2$. We used a generic method, previously validated, for quantifying the IVIM parameters. Results may have been different if software of specific vendors were used.

In conclusion, $D_{fast}$ is the best IVIM parameter in differentiating high- versus low-grade fibrosis. However, its usefulness is likely to be reduced by poor interobserver correlation. IVIM parameters are not strongly predictive of hepatic fat content or inflammatory activity.

## References


1. Falize Ludivine, Guillygomarc'h Anne, Perrin Michele, et al. (2006) Reversibility of hepatic fibrosis in treated genetic hemochromatosis: a study of 36 cases†. Hepatology 44(2):472–477
2. Marcellin P, Gane E, Buti M, et al. (2013) Regression of cirrhosis during treatment with tenofovir disoproxil fumarate for chronic hepatitis B: a 5-year open-label follow-up study. Lancet 9(381): 468–475
3. Ichikawa S, Motosugi U, Morisaka H, et al. (2015) MRI-based staging of hepatic fibrosis: comparison of intravoxel incoherent motion diffusion-weighted imaging with magnetic resonance elastography. J Magn Reson Imaging 42(1):204–210
4. Watanabe H, Kanematsu M, Goshima S, et al. (2011) Staging hepatic fibrosis: comparison of gadoxetate disodium–enhanced and diffusion-weighted MR imaging—preliminary observations. Radiology 259(1):142–150
5. Bohte AE, de Niet A, Jansen L, et al. (2014) Non-invasive evaluation of liver fibrosis: a comparison of ultrasound-based transient elastography and MR elastography in patients with viral hepatitis B and C. Eur Radiol 24(3):638–648
6. Haimerl M, Verloh N, Zeman F, et al. (2013) Assessment of clinical signs of liver cirrhosis using T1 mapping on Gd-EOB-DTPA-enhanced 3T MRI. PLoS ONE 8(12):e85658
7. Bakan AA, Inci E, Bakan S, Gokturk S, Cimilli T (2012) Utility of diffusion-weighted imaging in the evaluation of liver fibrosis. Eur Radiol 22(3):682–687
8. Taouli B, Tolia AJ, Losada M, et al. (2007) Diffusion-weighted MRI for quantification of liver fibrosis: preliminary experience. AJR Am J Roentgenol 189(4):799–806
9. Jajamovich GH, Calcagno C, Dyvorne HA, Rusinek H, Taouli B (2014) DCE-MRI of the liver: reconstruction of the arterial input function using a low dose pre-bolus contrast injection. PLoS ONE 9(12):e115667
10. Xu PJ, Yan FH, Wang JH, Lin J, Ji Y (2009) Added value of breathhold diffusion-weighted MRI in detection of small hepatocellular carcinoma lesions compared with dynamic contrast-enhanced MRI alone using receiver operating characteristic curve analysis. J Magn Reson Imaging 29(2):341–349
11. Bulow R, Mensel B, Meffert P, et al. (2013) Diffusion-weighted magnetic resonance imaging for staging liver fibrosis is less reliable in the presence of fat and iron. Eur Radiol 23(5):1281–1287
12. Sandrasegaran K, Akisik FM, Lin C, et al. (2009) Value of diffusion-weighted MRI for assessing liver fibrosis and cirrhosis. AJR Am J Roentgenol 193(6):1556–1560
13. Tosun M, Inan N, Sarisoy HT, et al. (2013) Diagnostic performance of conventional diffusion weighted imaging and diffusion tensor imaging for the liver fibrosis and inflammation. Eur J Radiol 82(2):203–207
14. Wang QB, Zhu H, Liu HL, Zhang B (2012) Performance of magnetic resonance elastography and diffusion-weighted imaging for the staging of hepatic fibrosis: a meta-analysis. Hepatology 56(1):239–247
15. Le Bihan DBE, Lallemand D, Grenier P, Cabanis E, Laval-Jeantet M (1986) MR imaging of intravoxel incoherent motions: application to diffusion and perfusion in neurologic disorders. Radiology 161:401–407
16. Koh DM, Collins DJ, Orton MR (2011) Intravoxel incoherent motion in body diffusion-weighted MRI: reality and challenges. AJR Am J Roentgenol 196(6):1351–1361
17. Chung SR, Lee SS, Kim N, et al. (2015) Intravoxel incoherent motion MRI for liver fibrosis assessment: a pilot study. Acta Radiol 56(12):1428–1436
18. Franca M, Marti-Bonmati L, Alberich-Bayarri A, et al. (2017) Evaluation of fibrosis and inflammation in diffuse liver diseases using intravoxel incoherent motion diffusion-weighted MR imaging. Abdom Radiol (NY) 42(2):468–477
19. Lu PX, Huang H, Yuan J, et al. (2014) Decreases in molecular diffusion, perfusion fraction and perfusion-related diffusion in fibrotic livers: a prospective clinical intravoxel incoherent motion MR imaging study. PLoS ONE 9(12):e113846
20. Luciani A, Vignaud A, Cavet M, et al. (2008) Liver cirrhosis: intravoxel incoherent motion MR imaging–pilot study. Radiology 249(3):891–899
21. Patel J, Sigmund EE, Rusinek H, et al. (2010) Diagnosis of cirrhosis with intravoxel incoherent motion diffusion MRI and dynamic contrast-enhanced MRI alone and in combination: preliminary experience. J Magn Reson Imaging 31(3):589–600
22. Wu CH, Ho MC, Jeng YM, et al. (2015) Assessing hepatic fibrosis: comparing the intravoxel incoherent motion in MRI with acoustic

radiation force impulse imaging in US. Eur Radiol 25(12):3552–3559
23. Yoon JH, Lee JM, Baek JH, et al. (2014) Evaluation of hepatic fibrosis using intravoxel incoherent motion in diffusion-weighted liver MRI. J Comput Assist Tomogr 38(1):110–116
24. Goffe WL, Ferrier GD, Rogers J (1994) Global optimization of statistical functions with simulated annealing. J Econom 60(1–2): 65–99
25. Bedossa P, Poynard T (1996) An algorithm for the grading of activity in chronic hepatitis C. The METAVIR Cooperative Study Group. Hepatology 24(2):289–293
26. Goodman ZD (2007) Grading and staging systems for inflammation and fibrosis in chronic liver diseases. J Hepatol 47(4):598–607
27. Girometti R, Furlan A, Bazzocchi M, et al. (2007) Diffusion-weighted MRI in evaluating liver fibrosis: a feasibility study in cirrhotic patients. Radiol Med 112:394–408
28. Lewin MP-RA, Boelle PY, et al. (2007) Diffusion-weighted magnetic resonance imaging for the assessment of fibrosis in chronic hepatitis C. Hepatology 46:658–665
29. Girometti RFA, Esposito G, et al. (2008) Relevance of b-values in evaluating liver fibrosis: a study in healthy and cirrhotic subjects using two single-shot spin-echo echo-planar diffusion-weighted sequences. J Magn Reson Imaging 28:411–419
30. Bonekamp S, Torbenson MS, Kamel IR (2011) Diffusion-weighted magnetic resonance imaging for the staging of liver fibrosis. J Clin Gastroenterol 45(10):885–892
31. Cece H, Ercan A, Yildiz S, et al. (2013) The use of DWI to assess spleen and liver quantitative ADC changes in the detection of liver fibrosis stages in chronic viral hepatitis. Eur J Radiol 82(8):e307–e312
32. Tosun M, Inan N, Sarisoy HT, et al. (2012) Diagnostic performance of conventional diffusion weighted imaging and diffusion tensor imaging for the liver fibrosis and inflammation. Eur J Radiol 82(2):203–207
33. Koinuma MOI, Hanafusa K, Shibuya H (2005) Apparent diffusion coefficient measurements with diffusion-weighted magnetic resonance imaging for evaluation of hepatic fibrosis. J Magn Reson Imaging 22(1):80–85
34. Chow AM, Gao DS, Fan SJ, et al. (2012) Liver fibrosis: an intravoxel incoherent motion (IVIM) study. J Magn Reson Imaging 36(1):159–167
35. Le Bihan D, Breton E, Lallemand D, et al. (1988) Separation of diffusion and perfusion in intravoxel incoherent motion MR imaging. Radiology 168:497–505
36. Zhang SX, Jia QJ, Zhang ZP, et al. (2014) Intravoxel incoherent motion MRI: emerging applications for nasopharyngeal carcinoma at the primary site. Eur Radiol 24(8):1998–2004
37. Andreou A, Koh DM, Collins DJ, et al. (2013) Measurement reproducibility of perfusion fraction and pseudodiffusion coefficient derived by intravoxel incoherent motion diffusion-weighted MR imaging in normal liver and metastases. Eur Radiol 23(2): 428–434
38. Kakite S, Dyvorne H, Besa C, et al. (2015) Hepatocellular carcinoma: short-term reproducibility of apparent diffusion coefficient and intravoxel incoherent motion parameters at 3.0T. J Magn Reson Imaging 41(1):149–156
39. Lee Y, Lee SS, Kim N, et al. (2015) Intravoxel incoherent motion diffusion-weighted MR imaging of the liver: effect of triggering methods on regional variability and measurement repeatability of quantitative parameters. Radiology 274(2):405–415
40. Li YT, Cercueil JP, Yuan J, et al. (2017) Liver intravoxel incoherent motion (IVIM) magnetic resonance imaging: a comprehensive review of published data on normal values and applications for fibrosis and tumor evaluation. Quant Imaging Med Surg 7(1):59–78
41. Hansmann J, Hernando D, Reeder SB (2013) Fat confounds the observed apparent diffusion coefficient in patients with hepatic steatosis. Magn Reson Med 69(2):545–552
42. Poyraz AK, Onur MR, Kocakoc E, Ogur E (2012) Diffusion-weighted MRI of fatty liver. J Magn Reson Imaging 35(5):1108–1111
43. Leporq B, Saint-Jalmes H, Rabrait C, et al. (2015) Optimization of intra-voxel incoherent motion imaging at 3.0 Tesla for fast liver examination. J Magn Reson Imaging 41(5):1209–1217